International Journal of Engineering Innovation & Research
Volume 11, Issue 5, ISSN: 2277 – 5668

Analysis of Influence of Structure Parameters on Output Performance of Combined Pole Permanent Magnet Generator

Jun Zhang[1], Yanhong Gao[1], Wei Wang[2*], Mingling Gao[3], Sizhan Hua[2] and Kai Geng[2]
[1]Shandong Tangjun Ouling Automobile Manufacturing Co. Ltd, Zibo City, Shandong Province, 255000, China.
[2]School of Transportation and Vehicle Engineering, Shandong University of Technology, Zibo City, Shandong Province, 255000, China.
[3]School of Computer Science and Technology, Shandong University of Technology, Zibo City, Shandong Province, 255000, China.
*Corresponding author email id: wangwei_sdut@163.com
Date of publication (dd/mm/yyyy): 04/09/2022

***Abstract* – The output voltage of the combined pole permanent magnet generator is mainly affected by the air gap magnetic density. Because the generator has stator slots and pole distances, there are harmonics in the air gap magnetic density and output voltage waveform, and the peak and sinusoidal characteristics of the waveform are not ideal. The radial distribution function of the air gap magnetic density is derived through the Carter coefficient, and the permanent magnet size, the shape of the magnetic separation slot the structure parameters such as air gap length and stator slot width are simulated and optimized, and the output characteristics of permanent magnet generator are compared with different parameter values to determine the optimal value of structure parameters, so as to improve the output performance of permanent magnet generator.**

***Keywords* – Combined Pole Permanent Magnet Generator, Radial Air Gap Magnetic Density, Simulation Optimization, Automobile.**

I. INTRODUCTION

With the improvement of scientific and technological level, light vehicles are more comfortable and intelligent, and the increase of on-board electrical equipment such as electric seats also puts forward higher requirements for the power supply system. As one of the main components of the automobile power supply system, the automobile generator converts mechanical energy into electrical energy through the rotation of the generator rotor driven by the engine, and provides DC power to the air conditioner, lamps and other electrical equipment on the vehicle, while charging the on-board battery [1, 2].

In recent years, many scholars have done some research on the rotor structure of generator and have made some research results. Reference [3] proposes a permanent magnet synchronous generator structure with an excitation winding added on the basis of the tangential arrangement of permanent magnets. The permanent magnets are connected in parallel with each other in the rotor core to provide the main magnetic flux of the motor. The excitation winding increases or decreases the air gap magnetic density through the forward current or the reverse current. The permanent magnet motor of this structure does not need a rectifying regulator, and the output voltage of the motor can be controlled by adjusting the magnitude of the excitation current. However, due to the existence of the excitation winding, the axial length of the motor increases, the loss increases, and the utilization rate of the pole surface of the permanent magnet is not high. Reference [4] proposes an axial permanent magnet synchronous generator with double rotor structure. The two rotor cores are located on both sides of the stator, the permanent magnets are fully utilized, the motor structure is simple and efficient, and the permanent magnets are easy to be cooled. However, the permanent magnet motor with this structure has a large

amount of permanent magnets, a large motor mass, and a large flux leakage of each pole permanent magnet steel.

The rotor of the combined pole permanent magnet generator is embedded in the rotor core in different radial or tangential ways compared to the traditional arrangement. There are more structural forms. Reference [5] proposes a new type of combined excitation permanent magnet generator structure with two kinds of permanent magnets arranged tangentially. The neodymium iron boron permanent magnet is installed outside the rotor core and the ferrite is installed inside the rotor core, the two permanent magnets of each pole jointly generate magnetic force lines to enter the air gap to reduce magnetic leakage and reduce the risk of irreversible demagnetization of neodymium iron boron. The output characteristics of the motor are good. However, the motor uses a large amount of permanent magnet materials, which increases the manufacturing cost. Moreover, the installation of permanent magnet materials is complex and requires high strength of the rotor core.

This paper presents a new type of combined magnetic pole permanent magnet generator. Each pole of the rotor of the generator is composed of two long rectangular permanent magnet steels and one annular permanent magnet steel. The rectangular permanent magnet steel and the annular permanent magnet steel work together to provide magnetic flux to the air gap, reduce magnetic leakage and achieve better magnetic concentration effect. The annular permanent magnet steel of each pole is located in the middle of the rectangular permanent magnet steel, which can reduce the harmonic in the magnetic density waveform of the air gap and improve its sinusoidity [6], Its structure is shown in Fig. 1.

Due to its complex structure and large number of permanent magnets, it is difficult to determine various parameters of the generator. In order to improve the sinusoidity of the air gap magnetic density, this paper proposes an optimization method. By solving the Carter coefficient of the generator and deriving the air gap magnetic density function of the generator, the structural parameters affecting the output performance of the generator are determined, and these structural parameters are individually optimized to improve the sinusoidity of the air gap magnetic density of the generator, Improve the output performance of the generator [7].

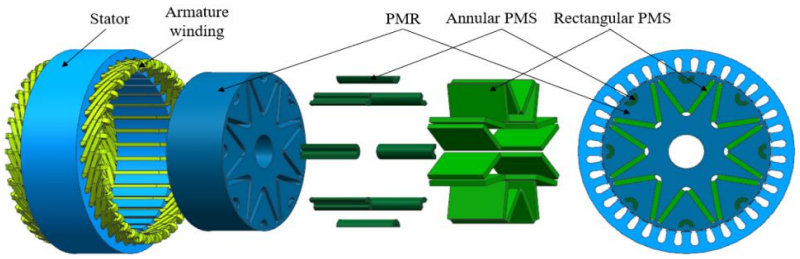

Fig. 1. Structure of combined pole permanent magnet generator.

II. Influencing Factors of Motor Output Performance

The permanent magnet generator is provided with air gap magnetic permeability by the permanent magnet embedded in the rotor. Affected by the cogging effect, there are harmonics in the air gap magnetic density waveform, which reduces the output performance of the generator. In order to study the influence factors on the sinusoidity of the air gap magnetic density waveform, the Carter coefficient can be used to calculate and analyze the influence factors of the air gap magnetic density of the permanent magnet generator. According to the Carter rule, in order to facilitate the calculation, it is assumed that [8]:

1. Ignoring the influence of motor curvature on the field distribution;
2. Ignoring the change of axial field distribution;
3. The pole width of the permanent magnet is infinite, and there is no pole leakage;
4. The groove is of infinite depth;
5. Permeability of teeth and yoke $\mu_{Fe}=\infty$;
6. Anisotropic permanent magnets are used and are uniformly magnetized to saturation in the easy magnetization direction;

The stator core is of 36 slots evenly distributed structure. It is only necessary to analyze the magnetic density distribution of a single slot, establish the physical model of the stator slot and analyze the magnetic density distribution between the stator teeth, as shown in Fig. 2.

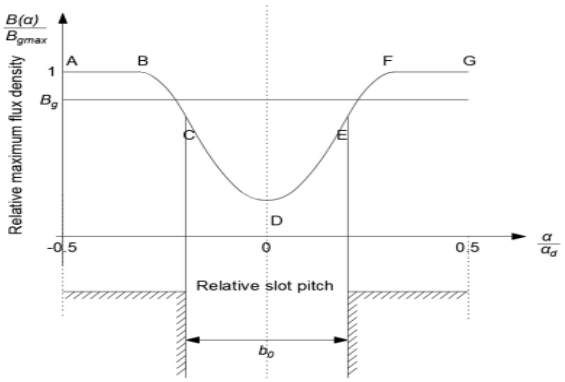

Fig. 2. The physical model of the stator slot and the distribution of the magnetic density.

It can be seen from Fig. 2 that the slot width of the stator slot is B_{s0}, the radius is r, and a circle is drawn in the air gap. The magnetic potential difference on the surface of the iron core is Ω_0. The magnetic density B of any point in the air gap between the stator slot and the generator is equal to the ratio of the magnetic potential difference Ω_0 at that point to the air gap magnetic resistance R:

$$B=\Omega_0/R \tag{1}$$

Where:

$$R=\frac{\delta}{\mu_0 A}=\frac{\delta}{\mu_0 L\left(y_s-K_{cs}w_s\right)} \tag{2}$$

In the formula, μ_0 —— vacuum permeability, δ ——axial length of the air gap, L ——radial length of the air gap, y_s —— distance between two adjacent slots, w_s ——width of the stator slot, K_{cs} ——Carter coefficient. Carter coefficient can be determined by the air gap magnetic density distribution within a slot pitch. As shown in Fig. 2, the slot width is B_{s0}, the maximum value of air gap magnetic density within a slot pitch is B_{max}, and the average value of air gap magnetic density within a slot pitch is B_g. It can be seen from the figure that the air gap magnetic density from point a to point B, from point F to point G is close to the maximum air gap magnetic density, and the minimum air gap magnetic density is located at the center line of the slot. Assuming that the

equivalent slot width is B_e, the magnetic density under the equivalent slot width is zero, and the magnetic density under the non equivalent slot width is the maximum, then there is

$$B_e = \xi B_{s0} \tag{3}$$

Where

$$\xi = \left[\frac{2}{\pi} \arctan \frac{B_{s0}}{2\delta} - \frac{2\delta}{B_{s0}} \ln \sqrt{1 + \left(\frac{B_{s0}}{2\delta} \right)^2} \right] \tag{4}$$

Carter coefficient is

$$K_{cs} = \frac{t}{t - \xi B_{s0}} \tag{5}$$

Where t is the ruler distance.

The formula (2), (4) and (5) are combined and brought into formula (1) to obtain,

$$B_r = \frac{\Omega_0 \mu_0 L}{\delta} \left\{ y_s - \frac{t \cdot w_s}{t - B_{s0} \cdot \left[\frac{2}{\pi} \arctan \frac{B_{s0}}{2\delta} - \frac{2\delta}{B_{s0}} \ln \sqrt{1 + \left(\frac{B_{s0}}{2\delta} \right)^2} \right]} \right\} \tag{6}$$

The magnetic flux generated by the permanent magnet directly enters the main air gap through the outer circle of the rotor. The permanent magnet is equivalent to a concentrated winding, which is the same as the calculation method of the rotor magneto motive force of the main air gap of the electric excitation magnetic field.

The magneto motive force F_{0p} generated by the permanent magnetic field is

$$F_{0p} = \frac{2 B_r h_{p1}}{\mu_p} \tag{7}$$

In the formula, h_{p1}——Length of tangential permanent magnet in magnetization direction, B_r——Permanent magnetic air gap magnetic density, μ_p——Permeability of permanent magnet.

The circumferential rotor magneto motive force $F_p(x)$ generated by the permanent magnetic field after Fourier transform in the main air gap is:

$$F_p(x) = \sum_{n=1}^{\infty} F_{np} \sin\left(\frac{n\pi}{\tau_s} x \right) \qquad n = 1, 3, 5, \cdots \tag{8}$$

In the formula, τ_s——Generator pole distance, F_{np}——N-th Fourier expansion coefficient.

$$F_{np} = (-1)^{\frac{n+3}{2}} \frac{4}{n\pi} F_{0p} \sin\left(\frac{n\pi\alpha_p}{2} \right) = (-1)^{\frac{n+3}{2}} \frac{8 B_r h_{p1}}{n\pi\mu_p} \sin\left(\frac{n\pi\alpha_p}{2} \right) \tag{9}$$

Where, α_p——pole arc coefficient of permanent magnet rotor.

Similarly, in polar coordinates, the radial magnetic density of the main air gap of the permanent magnet magnetic field ignoring the influence of the stator slot can be expressed as

$$B'_{pm}(r,\beta)=\sum_{v=1}^{\infty}(-1)^{\frac{v+3}{2}}\frac{8\mu_0\left(B_r h_p+B_r h_{pc}\right)}{\tau_s\mu_p}\frac{\mathrm{ch}\left[v\frac{\pi}{\tau_s}(\delta-r\sin\beta)\right]}{\mathrm{sh}\left(v\frac{\pi}{\tau_s}\delta\right)}\sin\left(\frac{v\pi\alpha}{2}\right)\sin\left(\frac{v\pi r\cos\beta}{\tau_s}\right) \tag{10}$$

Thus, it can be calculated that considering the influence of stator slot, under the polar coordinate, the axis of phase a winding is taken as the polar coordinate axis, the polar coordinate axis coincides with the center line of stator slot distance, and the N-pole axis of the rotor is located at the angular position. The radial component $B_r(r,\theta,\gamma)$ of the air gap magnetic field at the main air gap radius r of the hybrid excitation generator considering the influence of stator slot is expressed as:

$$B_r(r,\theta,\gamma)=\tilde{\lambda}(r,\theta)\left(B'_{em}(r,\theta-\gamma)+B'_{pm}(r,\theta-\gamma)\right) \tag{11}$$

It can be seen from equation (11) that the air gap magnetic density of the permanent magnet generator is related to several structural parameters. When the permanent magnet steel material, the inner and outer diameters of the stator and rotor cores, the number of stator slots and the number of motor poles have been determined through design and calculation, the size of the air gap magnetic density is related to the structural parameters such as the size of the permanent magnet steel, the length of the air gap and the width of the stator slot. The optimal value is determined through parameter optimization, reduce the air gap flux density and the harmonic content in the phase voltage waveform, improve its sinusoidity and improve the output performance of the permanent magnet generator [9].

III. Optimization of Electromagnetic Performance of Combined Pole Permanent Magnet Generator

The optimization of the electromagnetic performance of the combined pole permanent magnet generator is mainly based on the main influence parameters of the air gap magnetic field. According to the calculation in the previous section, the main parameters affecting the air gap magnetic field are the size of the permanent magnet, the structural parameters of the rotor core and the structural parameters of the stator core. The parametric modelling of the above three parameters is carried out to analyze their influence on the electromagnetic performance of the generator and calculate the optimal solution.

A. *Influence of Permanent Magnet Size on Motor Performance*

The magnetic flux of each pole of the permanent magnet generator is mainly provided by the rectangular permanent magnet steel with “V” shape on the inner side, and the small annular permanent magnet steel on the outer side mainly serves to gather magnetism and improve the sinusoidal waveform of the air gap magnetic density. Different dimensional parameters such as the magnetization direction length of the rectangular permanent magnet steel and the width of the permanent magnet are selected to analyze the influence on the output performance of the permanent magnet generator and determine the optimal parameter value.

(1) *Magnetization Direction Length of Permanent Magnet*

For the built-in combined pole permanent magnet generator of this design, the air gap magnetic density is mainly provided by the first rectangular permanent magnet steel with V-shape inside, so the parameters of the inner permanent magnet are mainly optimized. The shape and magnetization direction of the rectangular permanent magnet steel are shown in Fig. 3.

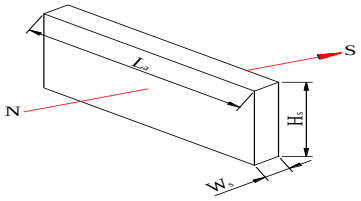

Fig. 3. Schematic diagram of rectangular permanent magnets.

In Fig. 3, N and s respectively represent two pole faces of the permanent magnet, W_s represents the magnetization direction length of the rectangular permanent magnet, H_s represents the width of the rectangular permanent magnet, and L_a represents the axial length of the rectangular permanent magnet.

The magnetization direction length W_s of the rectangular permanent magnet has a direct impact on the output performance of the generator, such as the magnetic flux density and the output voltage. This design mainly analyzes the influence of the two inner first rectangular permanent magnet steels on the generator performance. W_s is taken as 3 ~ 5mm, and 0.5mm is taken as a step. The relationship curve between different magnetization lengths of the permanent magnet and different performances of the generator is obtained by simulation, as shown in Fig. 4.

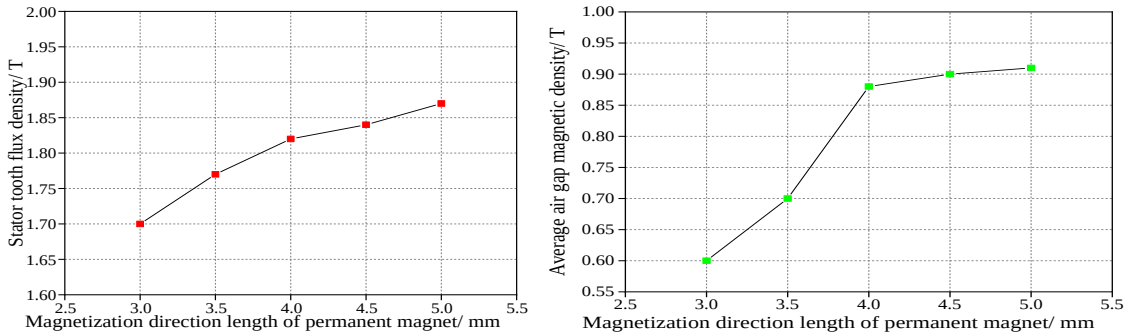

(a) Stator tooth magnetic density.

(b) Average air gap magnetic density.

Fig. 4. Influence of Magnetization Direction Length of the power generation device Magnetic Flux Density.

It can be seen from Fig. 4 that the magnetization direction length W_s of the permanent magnet increases from 3mm to 5mm, and the magnetic flux density of the stator teeth increases from 1.7T to 1.86T; However, the increase of the magnetization direction length of the permanent magnet has little effect on the average air gap magnetic density. The average air gap magnetic density of the generator is maintained between 0.6T and 0.91T, and when the W_s exceeds 4.5mm and continues to increase, the average air gap magnetic density has no obvious change.

The permanent magnet generator is simulated with different magnetization direction lengths of the permanent magnet, and the no-load phase voltage peak corresponding to the A-phase armature winding is shown in Fig. 5.

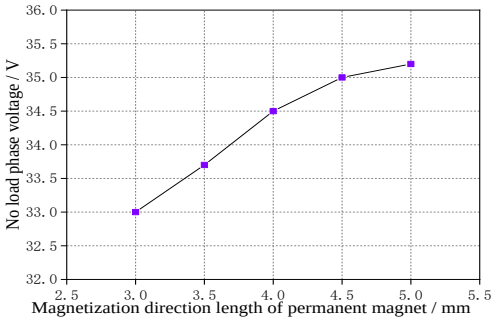

Fig. 5. The influence of permanent magnet magnetization direction length on the peak value of phase voltage of power generating device.

It can be seen from Fig. 5 that when the magnetization direction length of the rectangular permanent magnet gradually increases, the magnetic flux density generated by the rectangular permanent magnet increases, and the no-load output voltage of phase a of the permanent magnet generator during no-load operation also linearly increases. When the magnetization length of the permanent magnet increases to 5mm, the magnetic flux density of the stator teeth is nearly saturated, and the output voltage changes not significantly. Therefore, the magnetization direction length of the rectangular permanent magnet is taken as 5mm for the generator.

(1) *Width of Permanent Magnet*

The width H_s of the rectangular permanent magnet is simulated and analyzed to determine the optimal size of the V-shaped rectangular permanent magnet. In this paper, the permanent magnet width H_s is selected as 5 ~ 25mm, and the air gap magnetic density peak value, generator output voltage value and the third harmonic amplitude in the voltage waveform diagram of the permanent magnet generator under different permanent magnet widths are obtained as shown in Fig. 6.

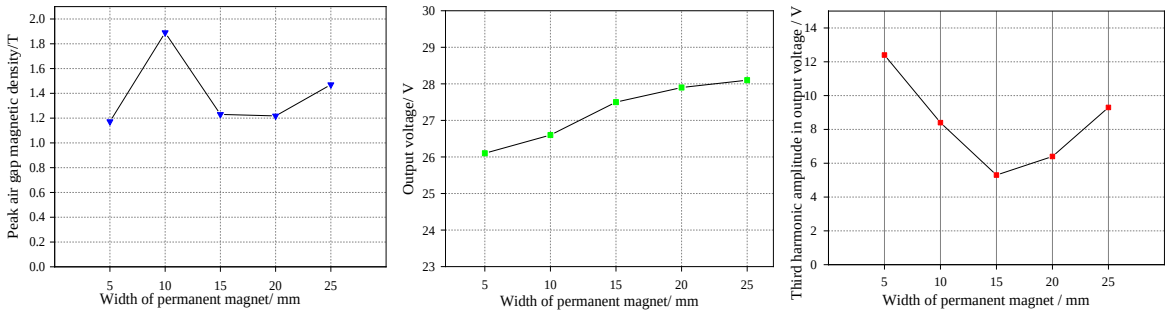

(a) Air gap magnetic density peak. (b) Output voltage value. (c) Third harmonic amplitude.

Fig. 6. Effect of permanent magnet width on power generation device simulation results.

It can be seen from Fig. 6 (a) that with the increase of the width of the permanent magnet steel, the peak value of the air gap magnetic density of the combined pole permanent magnet generator increases first and then decreases, and the maximum value appears when H_s = 15mm; As can be seen from figs. 6 (b) and 6 (c), with the increase of the width of the permanent magnet, the output voltage of the permanent magnet generator increases to about 27.6v. With the increase of the width of the permanent magnet, the voltage increase is not obvious; If the width of permanent magnet steel is too small or too large, the amplitude of the third harmonic in the armature reaction electromotive force is large, and the minimum value also appears at H_s = 15mm.

Therefore, the width H_s of the V-shaped rectangular permanent magnet was re selected as 15 mm.

A. *Influence of Rotor Core Structure Parameters on Motor Performance*

1. *Shape of Magnetic Isolation Groove*

For the permanent magnet generator of this design, most of the magnetic lines of force generated by the N pole of the permanent magnet enter the air gap and return to the S pole to form a complete magnetic circuit. The magnetic leakage mainly exists at the end of the permanent magnet. The magnetic lines of force generated by the n pole of the rectangular permanent magnet bypass the semi-circular magnetic separation groove and return to the S pole. In order to reduce the magnetic leakage, the shape of the magnetic separation groove at the end of the permanent magnet is changed and the simulation analysis is carried out. The simulation results are shown in Fig. 7.

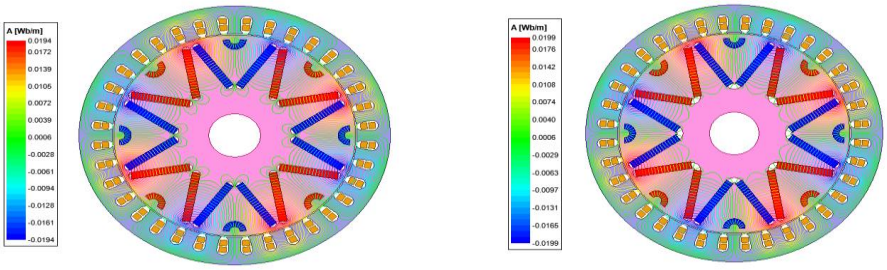

(a) Semicircular magnetic isolation groove. (b) Arc magnetic isolation groove.

Fig. 7. Distribution of magnetic force lines of power generation devices with different magnetic slots.

It can be seen from Fig. 7 that compared with the semi-circular magnetic separation groove, when the arc-shaped magnetic separation groove is adopted at the end of the first rectangular permanent magnet, its own leakage magnetic resistance is increased, the number of leakage magnetic lines at the end of the permanent magnet is significantly reduced, the generated magnetic lines of force better pass through the air gap and enter the stator core, the effective magnetic flux is increased, and the generator efficiency is improved.

In order to analyze the leakage flux density and air gap flux density of the generator at the end of the permanent magnet under different magnetic separation groove shapes, draw circles at the air gap and the arc-shaped magnetic separation groove at the end of the rectangular permanent magnet in the two-dimensional model of the generator respectively, and obtain the magnetic flux density waveforms at different positions, as shown in Fig. 8.

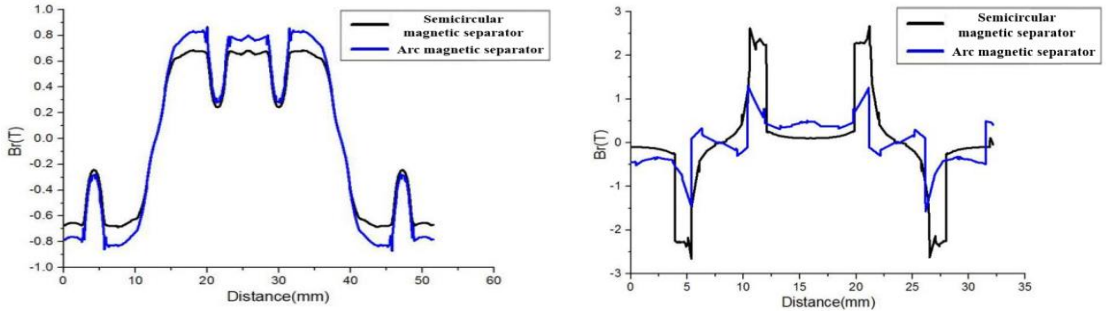

(a) Air gap magnetic density waveforms with different slot shapes.

(b) Flux leakage density waveforms at the end of permanent magnets with different slot shapes.

Fig. 8. Waveform diagrams of air gaps and magnetic flux density at the end of permanent magnets of different trough-shaped power generation devices.

It can be seen from Fig. 8 (a) that changing the shape of the magnetic separation groove at the end of the permanent magnet has little effect on the waveform of the air gap magnetic density of the generator. The waveforms of the air gap magnetic density of the two simulation results are nearly sinusoidal. However, when the optimized arc magnetic separation groove is adopted, the magnetic leakage at the end of the permanent magnet is reduced, and the peak value of the air gap magnetic density is increased from 0.7T to 0.8t. It can be seen from Fig. 8 (b) that after the arc-shaped magnetic separation groove is adopted, the magnetic leakage at the end of the rectangular permanent magnet is reduced, and the waveform peak of the magnetic leakage density is significantly lower than that of the semi-circular magnetic separation groove before optimization. Therefore, the arc-shaped magnetic separation groove is selected for the end of the rectangular permanent magnet of the combined pole permanent magnet generator in this design.

2. *Generator Air Gap Length*

Since the air gap magnetic density is affected by harmonics, the waveform diagram of the air gap magnetic density of the generator is not a standard sine wave. In order to improve the sinusoidity of the waveform, the non-uniform air gap of the generator can be realized by changing the parameters such as the thickness of the permanent magnet and the eccentric distance of the rotor [10]. The different realization methods of the non-uniform air gap are shown in Table 1.

Table 1. Different implementations of non-uniform air gaps.

Parameters	**Characteristic**	**Applicable Motor Type**
Thickness of permanent magnet	When the permanent magnets directly face the air gap, the permanent magnets of each pole change from equal thickness to unequal thickness, which changes the air gap length of the motor.	It is suitable for surface mounted permanent magnet generator, with high processing difficulty and cost.
Rotor eccentricity distance	The permanent magnet is placed inside the rotor core, and the outer surface shape of the rotor is changed by the eccentricity of the rotor, and the air gap length of the motor is changed.	Suitable for built-in permanent magnet generator, easy to process and widely used.

It can be seen from table 1 that in order to improve the magnetic density waveform of the air gap, the combined pole permanent magnet generator of this design realizes the non-uniform air gap by changing the eccentric distance of the rotor. The outer circle of the rotor of the traditional permanent magnet generator is a standard circle with O as the center. When the non-uniform air gap is adopted, the outer circle of the rotor is composed of eight arcs, and one arc is selected, with O_1 as the center. The distance h of OO_1 is the eccentric distance of the rotor. The larger the value of h, the larger the eccentric distance of the rotor, the greater the degree of non-uniformity of the air gap of the generator. The eccentric structure of the rotor is shown in Fig. 9.

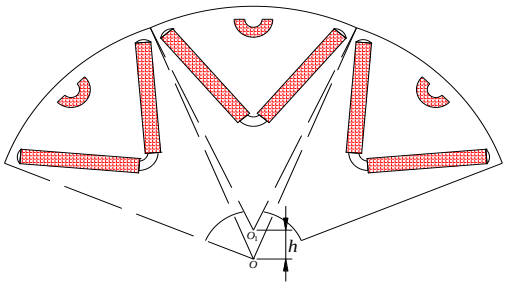

Fig. 9. Schematic diagram of rotor eccentric structure.

It can be seen from Fig. 9 that when the rotor eccentric structure is adopted, the air gap length at the upper end of the inner rectangular permanent magnet is the largest, and the magnetic resistance at the end is increased to reduce its own magnetic leakage. The air gap length at the end of the annular permanent magnet is the smallest. Reducing the magnetic resistance makes the magnetic force lines enter the air gap better, and the air gap magnetic density and phase voltage waveform of the generator are improved by changing the air gap length.

The air gap magnetic density and voltage waveform diagram of each phase obtained by the simulation of permanent magnet generator shall be standard sinusoidal waveform, and the waveform will be distorted under the influence of harmonics. The waveform distortion rate (THD) [11] is generally expressed by formula (12).

$$THD=\frac{\sqrt{U_2^2+U_3^2+U_4^2+\cdots+U_n^2}}{U_1}\times 100\% \tag{12}$$

In the formula, U_n —— The amplitude of the Nth harmonic.

It can be seen from formula (12) that the waveform distortion rate can be calculated by the amplitude value of each harmonic wave, and the peak value and waveform distortion rate of the air gap magnetic density and phase voltage of the generator under non-uniform air gap can be obtained by selecting the eccentricity *h* of different sizes, as shown in Fig. 10.

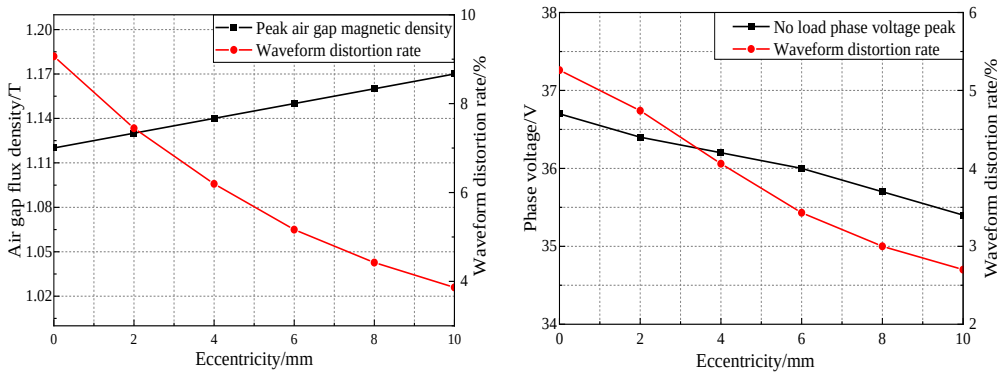

(a) Air gap magnetic density. (b) Phase voltage.

Fig. 10. Analysis of the influence of eccentricity on the peak value and distortion rate of the air gap magnetic density and phase voltage waveform.

It can be seen from Fig. 10 (a) and Fig. 10 (b) that with the increase of the rotor eccentricity, the air gap mag--netic density and the distortion rate of the phase voltage waveform are significantly reduced, which proves that the use of non-uniform air gap can effectively reduce harmonics and reduce the waveform distortion rate. When *h* is taken from 0 to 10mm, with the increase of the average air gap length of the generator, the peak value of air gap magnetic density will also increase from 1.12T to about 1.17T. However, as the reluctance of the motor increases, the peak value of no-load phase voltage will also decrease from 36.7V to 35.4V. Considering the influence of eccentricity on air gap magnetic density and phase voltage, *h* = 6mm is taken.

The simulation models of uniform air gap and non-uniform air gap permanent magnet generators are established respectively. Draw a circle in the air gap for simulation analysis to obtain the harmonic analysis diagram of generator air gap magnetic density before and after rotor eccentricity, as shown in Fig. 11.

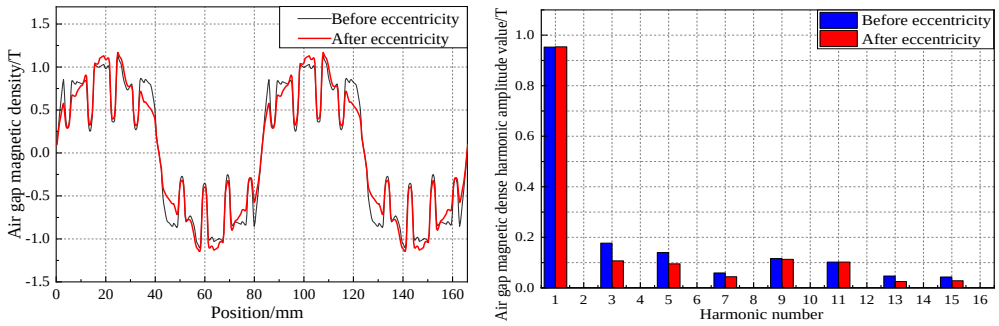

(a) Waveforms of air gap magnetic density before and after eccentricity.

(b) Amplitude value of each harmonic wave in air gap magnetic density waveform before and after eccentricity.

Fig. 11. The air-gap magnetic density waveform and odd harmonic analysis diagram of the power generation device before and after the eccentricity.

It can be seen from Fig.11 that the sinusoidity of the air gap magnetic density waveform is reduced by the influence of odd harmonics. After the eccentricity of the permanent magnet rotor, the sinusoidity of the waveform is better, and the amplitude values of the 3rd, 5th and 7th harmonics are significantly reduced. According to formula (12), the waveform distortion rate *(THD)* of the air gap magnetic density waveform after eccentricity is reduced by about 43.6% compared with that before eccentricity, which proves that the non-uniform air gap can effectively reduce the influence of harmonics on the air gap magnetic density waveform.

The simulation models of uniform air gap and non-uniform air gap permanent magnet generators are established respectively, and the A-phase armature winding is selected to obtain the no-load phase voltage harmonic analysis diagram before and after rotor eccentricity, as shown in Fig. 12.

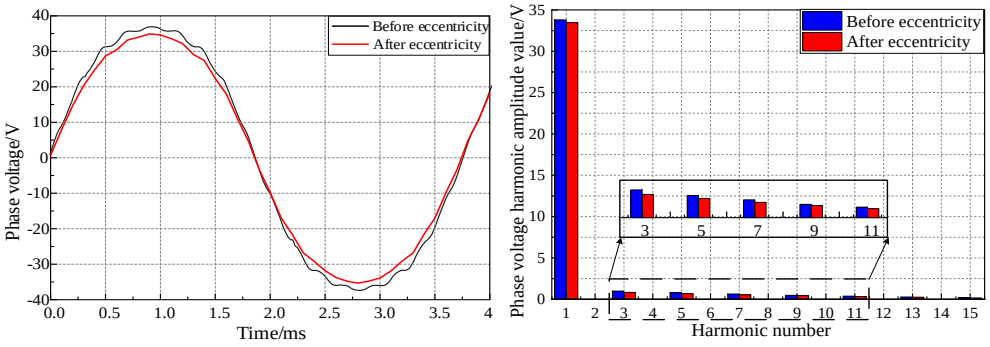

Fig. 12. Harmonic analysis diagram of no-load phase voltage of A-phase winding before and after eccentricity.

It can be seen from Fig. 12 that after the non-uniform air gap is adopted, the peak value of the no -load phase voltage of the generator is slightly reduced, but the whole waveform diagram is smoother and the fluctuation is reduced, and the amplitude values of the 3rd, 5th and 7th harmonics that affect the sine of the waveform are also reduced. The waveform distortion rate *(THD)* calculated by substituting the amplitude of each harmonic into formula (12) is reduced by about 96.07% compared with that before eccentricity. Therefore, when the non-uniform air gap with eccentricity h = 6mm is adopted in this design, the structure of the permanent magnet generator is reasonable and the harmonic content in the waveform diagram is reduced.

A. *Influence of Stator Core Structure Parameters on Motor Performance*

The slot width of the stator core will affect the distribution of the air gap magnetic density and the stator tooth

magnetic density of the generator, resulting in the change of its output voltage [12]. Here, the slot width is selected as 1 ~ 5mm, and the phase voltage and cogging torque peak of the permanent magnet generator under different slot widths are simulated as shown in Fig. 13.

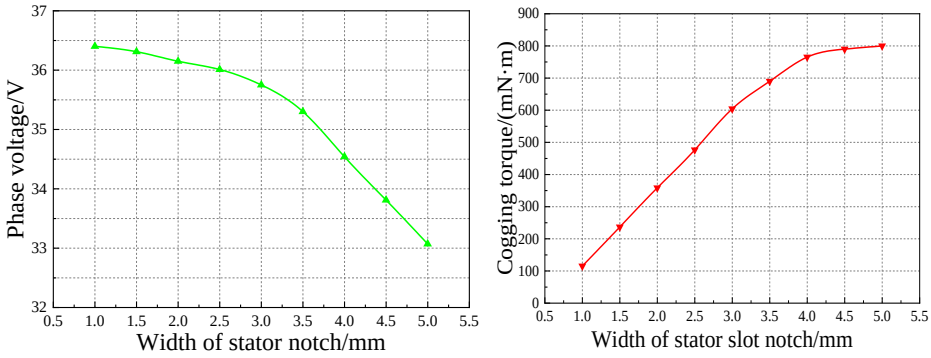

(a) Phase voltage peak. (b) Cogging torque peak.

Fig. 13. Peak diagrams of phase voltage and cogging torque of the power generation device under different slot widths.

It can be seen from Fig. 13 (a) that when the width of the stator slot increases, the proportion of the stator teeth decreases, and the stator teeth have reached saturation when the magnetic force lines in the air gap do not fully enter. According to the output voltage of the A-phase armature winding of the permanent magnet generator, the peak value of the no-load phase voltage of the A-phase winding also decreases; It can be seen from Fig. 13 (b) that when the width of the stator slot increases, the cogging effect of the permanent magnet generator during operation becomes larger, and the peak value of cogging torque becomes larger, which affects the output performance of the permanent magnet generator.

According to the simulation results in Fig. 13, the slot width of the stator should be selected as the middle value. If it is too large or too small, the output performance of the permanent magnet generator will be affected. The slot width B_{s0} is selected as 1.5mm, 2.5mm and 4.0mm. The harmonic content in the air gap magnetic density of the generator is obtained through simulation analysis, as shown in Fig. 14.

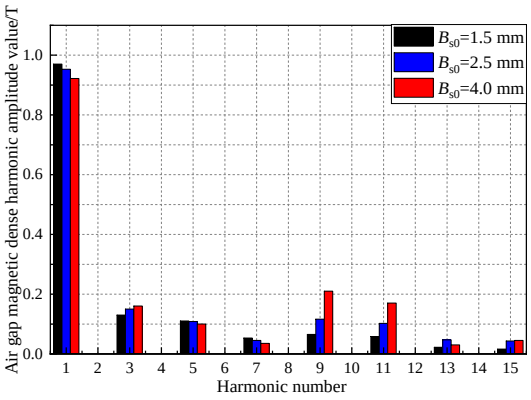

Fig. 14. Diagram of the odd harmonic content in the air gap magnetic density of the power generation device under different slot widths.

It can be seen from Fig.14 that when the slot width takes different parameter values, the amplitude values of the 3rd, 5th, 9th and 11th harmonic waves in the no-load air gap magnetic density waveform diagram of the generator are larger. The statistics of the amplitude values of the 3rd, 5th, 9th and 11th harmonic waves are shown in Table 2.

Table 2 3, 5, 9 and 11 harmonic amplitude table in the air gap magnetic density waveform.

Harmonic amplitude order / Notch width	3rd	5th	9th	11th
1.5mm	1.64T	1.01T	0.63T	0.61T
2.5mm	1.53T	1.00T	1.08T	0.99T
4.0mm	1.76T	0.98T	2.03T	1.78T

It can be seen from Table 2 that when the stator slot width is too large, the odd harmonic amplitude in the air gap magnetic density waveform diagram of the permanent magnet generator is large, and the sine of the waveform is poor. Therefore, the smaller the stator slot width, the better the output performance of the generator. However, if the slot width is too small, it will increase the difficulty of embedding the armature winding and increase the production cost of the prototype. The stator slot width B_{s0} in this design is taken as 2.5mm.

According to formula (11), the influence of structural parameters such as the length of permanent magnet magnetization direction, the width of permanent magnet, the length of air gap, the shape of permanent magnet magnetic separation slot, and the width of stator slot on the output performance of permanent magnet generator is analyzed. The size of structural parameters determined through simulation and optimization is shown in Table 3.

Table 3. The initial design dimensions of permanent magnet power generation device.

Structural Parameters	**Numerical Value**
Magnetization direction length of rectangular permanent magnet (mm)	5
Width of rectangular permanent magnet (mm)	15
Rotor eccentricity distance(mm)	6
Shape of magnetic isolation groove	Curve
Width of stator slot (mm)	2.5

The air gap magnetic density and phase voltage waveform diagram are obtained by simulation of the combined pole permanent magnet generator with optimized structure, and the comparison with the simulation results of the generator before optimization is shown in Fig. 15.

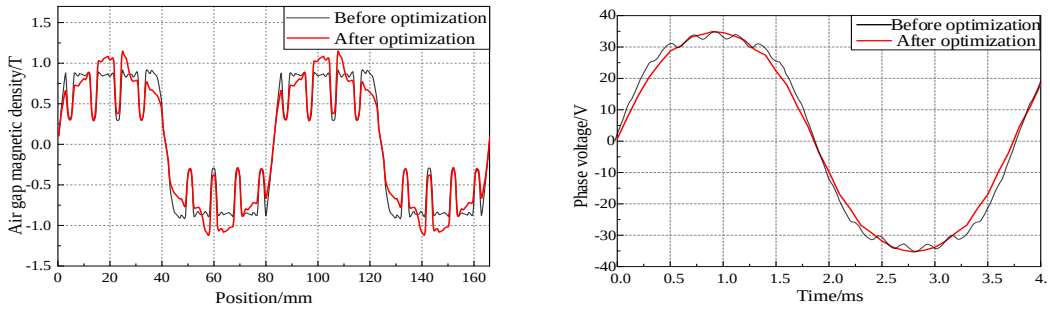

(a) Preferred front and rear air gap magnetic density waveform (b) Preferred front and rear phase voltage waveform diagram

Fig. 15. Waveforms of air gap magnetic density and phase voltage before and after structure optimization of permanent magnet generator.

It can be seen from Fig. 15 (a) that after the optimization of the generator structure, the peak value of the air gap magnetic density becomes larger and the waveform sine is better. This is because the leakage of the permanent magnet decreases and the effective magnetic flux entering the air gap increases. At the same time, by comparing the waveforms before and after optimization, it can be seen that the average value of air gap magnetic density is 0.71T, which is higher than the 0.65T before optimization; It can be seen from Fig. 15 (b) that after the structure optimization of the permanent magnet generator, the no-load phase voltage waveform of the A-phase armature winding is better sinusoidal, and the waveform distortion caused by harmonics is significantly reduced, which can provide a more stable output voltage for the electrical equipment of light vehicles.

When the generator is running, the cogging torque generated by cogging effect will affect the output characteristics of the generator and reduce its output efficiency [13]. The cogging torque comparison before and after the structural optimization of the combined pole permanent magnet generator is shown in Fig. 16 through simulation.

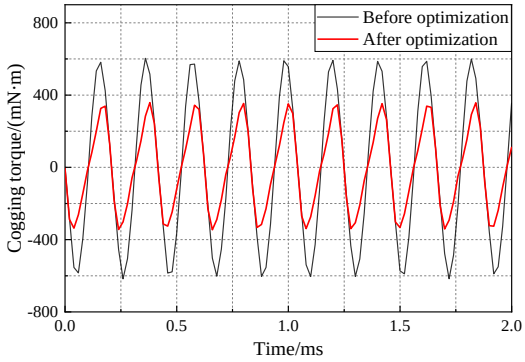

Fig. 16. Comparison diagram of generator cogging torque before and after optimization.

It can be seen from Fig.16 that the amplitude of the cogging torque before the optimization of the permanent magnet generator structure is large, and the maximum value can reach 600mN·m. after the optimization, the waveform amplitude of the cogging torque of the motor decreases, and the maximum value also decreases to 362mN·m. Therefore, it can be seen that the harmonic contained in the air gap magnetic density of the generator after the structure optimization is reduced, the waveform is better, the cogging effect of the motor is weakened, the output characteristic is improved, and the efficiency is higher.

IV. CONCLUSION

In this paper, a structure of combined pole permanent magnet generator is proposed, and the radial distribution function of air gap magnetic density of combined pole permanent magnet generator is derived by solving Carter coefficient, and the factors affecting the performance of the generator are determined. The effects of the structural parameters of the permanent magnet generator, such as the magnetization direction length of the permanent magnet, the width of the permanent magnet, the shape of the permanent magnet spacer slot, the length of the air gap and the width of the stator slot, on its output performance are analyzed, to obtain the optimal parameters. The structure shows that after optimization, the air gap flux density and the harmonic content in the phase voltage waveform diagram of the permanent magnet generator are reduced, and the sinusoidity is improved. The waveform distortion rate *(THD)* is reduced by about 96.07% compared with that

before optimization, and the cogging torque is reduced by about 40% compared with that before optimization, which improves the output performance of the permanent magnet generator.

REFERENCES

[1] SHI Liwei, Zhang Shaohong, Zhang Xueyi. Automotive electrical appliances [M]. Beijing: National defense industry press, 2011, 04: 254.
[2] MA Youliang. Automotive Electrical and electronic control system [M]. Beijing: China Machine Press, 2020, 01: 505.
[3] Zhang Z, Yan Y, Yang S, et al. Principle of Operation and Feature Investigation of a New Topology of Hybrid Excitation Synchronous Machine [J]. IEEE Transactions on Magnetics, 2008, 44(9):2174-2180.
[4] Zhang Z, Yan Y, Yang S, et al. Principle of Operation and Feature Investigation of a New Topology of Hybrid Excitation Synchronous Machine [J]. IEEE Transactions on Magnetics, 2008, 44(9):2174-2180.
[5] Zhu X , Xue W, Chao Z , et al. Design and analysis of a spoke-type hybrid permanent magnet motor for Electric Vehicles [J]. IEEE Transactions on Magnetics, 2017, PP(11):1-1.
[6] LI Zhongming. Rare earth permanent magnet motor [M]. Beijing: National Defense Industry Press, 1999, 07: 15-22.
[7] An Zhiwen. Design of permanent magnet synchronous motor for electric vehicle [J]. Journal of Physics: Conference Series, 2021, 1881(2).
[8] Shoji Isobe, Masakatsu Takemoto. Carter coefficient of iron core with magnetic wedge for rotating machinery [J]. Electrical Engineering in Japan,1986,106(6).
[9] Xu Zhiyu, Deng Zhiquan, Zhang Zhongming, et al. Analysis of influence of the inner diameter of the permanent magnet on rotor stress and critical speed for the high speed Permanent magnet motor [J]. Science Discovery, 2018, 6(5).
[10] Zhang Wenchao,Shi Liwei,Liu Kaiwen,Li Lintao,Jing Jianning. Optimization Analysis of Automotive Asymmetric Magnetic Pole Permanent Magnet Motor by Taguchi Method[J]. International Journal of Rotating Machinery, 2021, 2021.
[11] Xueyi Zhang,Qinjun Du,Jinbin Xu,et al. Development and analysis of the magnetic circuit on double-radial permanent magnet and salient-pole electromagnetic hybrid excitation generator for vehicles [J]. Chinese Journal of Mechanical Engineering, 2019, 32(02): 100-112.
[12] Rong chuanbing, Shen baogen. Nanocrystalline and nanocomposite permanent magnets by melt spinning technique [J]. Chinese Physics B, 2018, 27(11):5-58.
[13] Chen Zhongxian, Li Guanglin. A V type permanent magnet motor simulation analysis and prototype test for electric vehicle [J]. IEEE Access, 2019, 7.

AUTHOR'S PROFILE

First Author
Jun Zhang, Male, Shandong Tangjun Ouling Automobile Manufacturing Co. Ltd, Zibo City, Shandong Province, 255000, China. emailid: 25481500@qq.com

Second Author
Yanhong Gao, Female,Shandong Tangjun Ouling Automobile Manufacturing Co. Ltd, Zibo City, Shandong Province, 255000, China. emailid: 15275955717@126.com

Third Author
Wei Wang, Male, Master in reading (Correspondence author), School of Transportation and Vehicle Engineering, Shandong University of Technology, Shandong, Zibo, 255000, China.

Fourth Author
Mingling Gao, Female, Associate Professor, School of Computer Science and Technology, Shandong University of Technology, Shandong, Zibo, 255000, China. emailid: gml_3437@sina.com

Fifth Author
Sizhan Hua, Male, Master in reading, School of Transportation and Vehicle Engineering, Shandong University of Technology, Shandong, Zibo, 255000, China. emailid: hua17860911424@163.com

Sixth Author
Kai Geng, Male, Master in reading, School of Transportation and Vehicle Engineering, Shandong University of Techno--logy, Shandong, Zibo, 255000, China. emailid: gk17853118226@163.com